

Observer backstepping control of DFIG-Generators for wind turbines variable-speed: FPGA-based implementation



Badre Bossoufi ^{a, b, *}, Mohammed Karim ^b, Ahmed Lagrioui ^b, Mohammed Taoussi ^b, Aziz Derouich ^c

^a Laboratory of Electrical Engineering and Maintenance, Higher School of Technology, EST-Oujda, University of Mohammed I, Morocco

^b STIC Team, Faculty of Sciences Dhar El Mahraz, Sidi Mohamed Ben Abdellah University, Fez, Morocco

^c Laboratory of Electrical Engineering and Maintenance, Higher School of Technology, EST-Fez, Sidi Mohamed Ben Abdellah University, Fez, Morocco

ARTICLE INFO

Article history:

Received 19 March 2014

Accepted 3 April 2015

Available online

Keywords:

DFIG-Generator
Backstepping control
Adaptative control
Wind turbine
MPPT
FPGA

ABSTRACT

In this paper, we present a new contribution for the control of Wind-turbine energy systems, a nonlinear robust control of active and reactive power by the use of the Adaptative Backstepping approach based in double-fed asynchronous generator (DFIG-Generator).

Initially, a control strategy of the MPPT for extraction of maximum power of the turbine generator is presented. Thereafter, a new control technique for wind systems is presented. This control system is based on an adaptive pole placement control approach integrated to a Backstepping control system. The stability of the system is shown using Lyapunov technique. Using the FPGA to implement the order gives us a better rapidity. A Benchmark was realized by a prototyping platform based on DFIG-generator, FPGA and wind-turbine; the experimental results obtained show the effectiveness and the benefit of our contribution.

© 2015 Elsevier Ltd. All rights reserved.

1. Introduction

Today, wind energy has become a viable solution for the production of energy, in addition to other renewable energy sources. While the majority of wind turbines are fixed speed, the number of variable speed wind turbines is increasing [1]. The *Doubly-Fed Asynchronous Generator (DFIG)* with Backstepping control is a machine that has excellent performance and is commonly used in the wind turbine industry [2,3]. There are many reasons for using the Doubly-Fed Asynchronous Generator (DFIG) for wind turbine a variable speed, such as reducing efforts on mechanical parts, noise reduction and the possibility of control of active power and reactive.

The wind system using DFIG generator and a “back-to-back” converter that connects the rotor of the generator and the network has many advantages. One advantage of this structure is that the power converters used are dimensioned to pass a fraction of the

total system power [5,6]. This allows reducing losses in the power electronics components. The performances and power generation depends not only on the DFIG generator, but also the manner in which the two parts of “back-to-back” converter are controlled.

The power converter machine side is called “Rotor Side Converter” (RSC) and the converter Grid-side power is called “Grid Side Converter” (GSC). The RSC converter controls the active power and reactive power produced by the machine. As the GSC converter, it controls the DC bus voltage and power factor network side.

The speed performance of new components and the flexibility inherent of all programmable solutions give today many opportunities in the field of digital implementation for control systems. This is true for software solutions as microprocessor or DSP (Digital Signal Processor). However, specific programmable hardware technology such as Field Programmable Gate Array (FPGA) can also be considered as an especially appropriate solution in order to boost performances of controllers [1–3]. Indeed, these generic components combine low cost development, thanks to their re-configurability, use of convenient software tools and more and more significant integration density [4,5].

The FPGA technology is now used by an increasing number of designers in various fields of application such as signal processing [6], telecommunication, video, embedded control systems, and

* Corresponding author. Université Mohammed I, Ecole Supérieure de Technologie, Complexe Universitaire Al Qods, 60000 Oujda, Morocco. Tel.: +212 663 48 40 13.

E-mail address: badre_isai@hotmail.com (B. Bossoufi).

electrical control systems. This last domain, i.e. the studies of control of electrical machines, will be presented in this paper. Indeed, these components have already been used with success in many different applications such as Pulse Width Modulation (PWM), control of induction machine drives and multimachine system control.

This paper presents the realization of a platform for *adaptive Backstepping* control of *Wind turbine system based in DFIG-Generator* using *FPGA* based controller. This realization is especially aimed for future high performance applications. In this approach, not only the architecture corresponding to the control algorithm is studied, but also architecture and the *ADC* interface and *RS232 UART* architecture.

The adaptive backstepping approach offers a choice of design tools for accommodation of uncertainties nonlinearities. And can avoid wasteful cancellations. However, the not adaptive backstepping approach is capable of keeping almost all the robustness properties of the mismatched uncertainties. The not adaptive backstepping is a rigorous and procedure design methodology for nonlinear feedback control. The principal idea of this approach is to recursively design controllers for machine torque constant uncertainty subsystems in the structure and “step back” the feedback signals towards the control input. This approach is different from the approach of the conventional feedback linearization in that it can avoid cancellation of useful nonlinearities in pursuing the objectives of stabilization and tracking. A nonlinear backstepping control design scheme is developed for the speed tracking control of DFIG that has exact model knowledge. The asymptotic stability of the resulting closed loop system is guaranteed according to Lyapunov stability theorem.

The Backstepping control is a systematic and recursive design methodology for nonlinear feedback control. Applying those design methods, control objectives such as position, velocity can be achieved.

A nonlinear backstepping control design scheme is developed for the speed tracking control of DFIG that has exact model knowledge. The asymptotic stability of the resulting closed loop system is guaranteed according to Lyapunov stability theorem.

In this paper, we present a technique to control two power converters which is based on the backstepping control. We analyze their dynamic performances by simulations in Matlab/Simulink environment. We start by modeling of the wind turbine, and then a

tracking technique operating point at maximum power point tracking (MPPT) will be presented. Thereafter, we present a model of the DFIG in the dq reference, and the general principle of control of both power converters which is based on backstepping technique, Finally, the principle of the implementation on the FPGA target and source program Xilinx System Generator, and the test benchmark for the experimental validation of the proposed model in my lab work.

Considering the complexity of the diversity of the electric control devices of the machines, it is difficult to define with universal manner a general structure for such systems. However, by having a reflexion compared to the elements most commonly encountered in these systems, it is possible to define a general structure of an electric control device of machines which is show in Fig. 1:

2. Modelling of the wind-turbine

The model of the turbine is modeled from the following system of equations [7,8]:

$$P_{incident} = \frac{1}{2} \cdot \rho \cdot S \cdot v^3 \tag{1}$$

$$P_{extracted} = \frac{1}{2} \cdot \rho \cdot S \cdot C_p(\lambda, \beta) \cdot v^3 \tag{2}$$

$$\lambda = \frac{\Omega_t \cdot R}{v} \tag{3}$$

$$C_p^{max}(\lambda, \beta) = \frac{16}{27} \approx 0.593 \tag{4}$$

$$C_p(\lambda, \beta) = c_1 \cdot \left(c_2 \cdot \frac{1}{\lambda} - c_3 \cdot \beta - c_4 \right) \cdot e^{-c_5 \frac{1}{\lambda}} + c_6 \cdot \lambda \tag{5}$$

$$\frac{1}{A} = \frac{1}{\lambda + 0.08 \cdot \beta} - \frac{0.035}{1 + \beta^3} \tag{6}$$

$$C_{al} = \frac{P_{eol}}{\Omega_t} = \frac{1}{2} \cdot \rho \cdot S \cdot C_p(\lambda, \beta) \cdot v^3 \cdot \frac{1}{\Omega_t} \tag{7}$$

$$J = \frac{J_{tur}}{G^2} + J_g \tag{8}$$

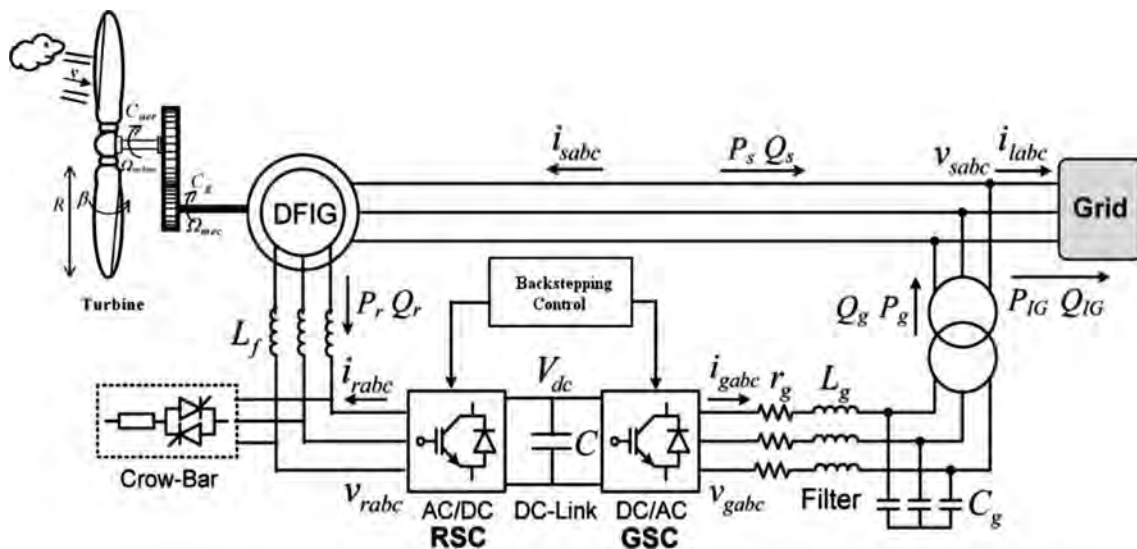


Fig. 1. Architecture of the control.

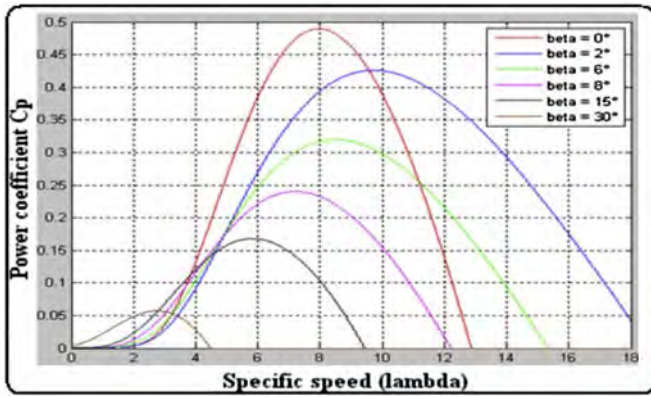


Fig. 2. Power coefficient as a function of λ and β .

$$J \frac{d\Omega_{mec}}{dt} = C_{mec} = C_{ar} - C_{em} - f \cdot \Omega_{mec} \quad (9)$$

- S: the area swept by the pales of the turbine [m^2]
- ρ : the density of the air ($\rho = 1.225 \text{ kg/m}^3$ at atmospheric pressure).
- V: wind speed [m/s]
- $C_p(\lambda, \beta)$: the power coefficient.
- λ : the specific speed
- β : the angle of orientation of the blades
- $P_{extracted}$: the power extracted of the turbine.
- Ω_t : Rotational speed of the turbine
- C_{al} : Torque on the slow axis (turbine side)
- J_{tur} : turbine inertia
- J_g : inertia of the generator.
- Ω_{mec} : Mechanical speed of DFIG
- C_{ar} : Aerodynamic torque on the fast axis of the turbine

$$c_1 = 0.5872, c_2 = 116, c_3 = 0.4, c_4 = 5, c_5 = 21, c_6 = 0.0085$$

The six coefficients c_1, c_2, c_3, c_4, c_5 are modified for maximum C_p equal to 0.564 for $\beta = 0^\circ$.

Fig. 2 shows the evolution of the power coefficient as a function of λ for different values of β . A coefficient of maximum power of $C_p = 0.564$ is obtained for a speed ratio λ which is (3) (λ_{opt}). Fixing β and λ respectively to their optimal values, the wind system provides optimal power (Fig. 3).

The above equations are used to prepare the block diagram of the model of turbine (Fig. 4).

3. Extraction of maximum power (MPPT control)

In order to capture the maximum power of the incident energy of the wind-turbine, must continuously adjust the rotational speed of the wind turbine. The optimal mechanical turbine speed corresponds has λ_{opt} and $\beta = 0^\circ$. The speed of the DFIG is used as a reference value for a controller proportional-integral type (PI phase advance). The latter determines the control set point which is the electromagnetic torque that should be applied to the machine to run the generator at its optimal speed.

The “Pitch Control” is a technique that mechanically adjusts the blade pitch angle to shift the curve of the power coefficient of the turbine [13].

However, it is quite expensive and is generally used for wind turbines and high average power. For our model, the “Stall Control” technique, which is a passive technique that allows a natural aerodynamic stall (loss of lift when the wind speed becomes more important). La régulation de la vitesse de rotation de l’angle de pas des pales de la turbine se produit lorsque la vitesse de la génératrice est supérieure à 30% de sa vitesse nominale. Otherwise, β is zero. The synthesis of the PI controller requires knowledge of the transfer function of our system. This is especially difficult because of the power coefficient. A simple proportional correction (P) is obtained after testing. Note that β may vary from 0° to 90° characterized by saturation (Fig. 5).

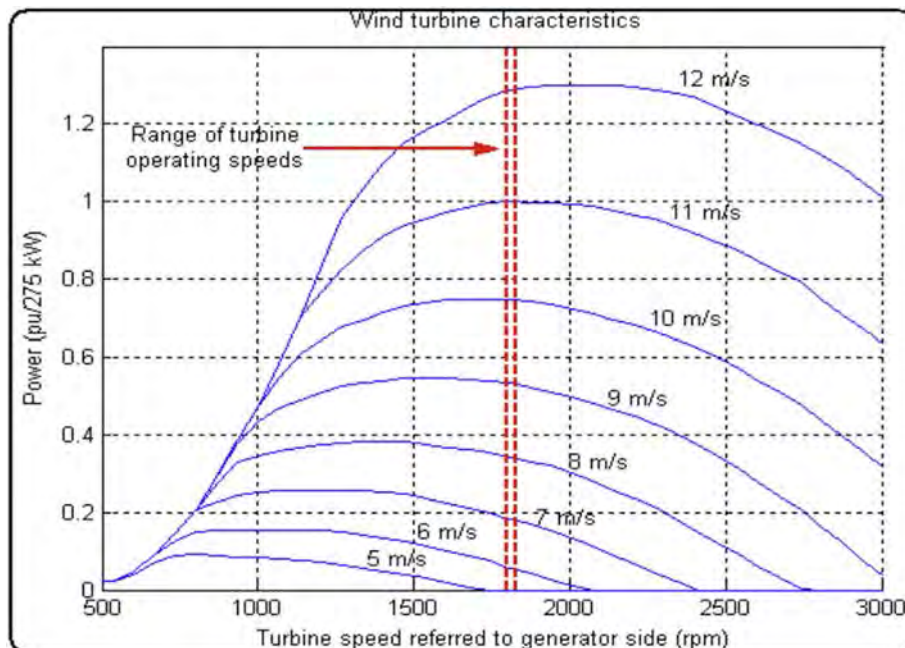


Fig. 3. Wind-turbine DFIG characteristics.

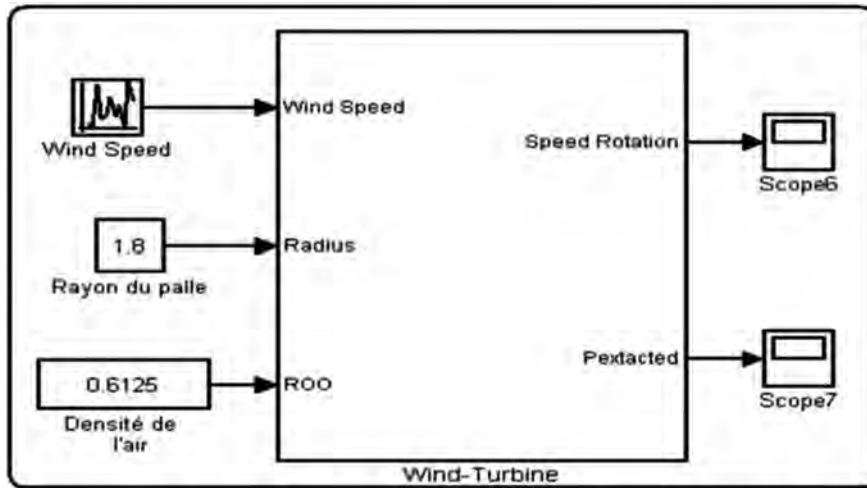


Fig. 4. Wind-turbine model.

4. DFIG model system

The Power equations in the d-q reference DFIG can be written [10–14]:

$$\begin{cases} v_{ds} = R_s \cdot i_{ds} + \frac{d}{dt} \phi_{ds} - \omega_s \cdot \phi_{qs} \\ v_{qs} = R_s \cdot i_{qs} + \frac{d}{dt} \phi_{qs} + \omega_s \cdot \phi_{ds} \\ v_{dr} = R_r \cdot i_{dr} + \frac{d}{dt} \phi_{dr} - \omega_r \cdot \phi_{qr} \\ v_{qr} = R_r \cdot i_{qr} + \frac{d}{dt} \phi_{qr} + \omega_r \cdot \phi_{dr} \end{cases} \quad (10)$$

with:

$$\begin{cases} \omega_r = \omega_s - P \cdot \Omega \\ \phi_{ds} = L_s \cdot i_{ds} + M \cdot i_{dr} \\ \phi_{qs} = L_s \cdot i_{qs} + M \cdot i_{qr} \\ \phi_{dr} = L_r \cdot i_{dr} + M \cdot i_{ds} \\ \phi_{qr} = L_r \cdot i_{qr} + M \cdot i_{qs} \\ L_s = l_s - M_s, L_r = l_r - M_r \end{cases} \quad (11)$$

L_s, L_r : Cyclic inductances of stator and rotor phase;
 l_s, l_r : Inductances of stator and rotor phase;
 M_s, M_r : Mutual inductances between stator and rotor phases respectively;
 M : Maximum mutual inductance between stator and rotor stage (the axes of the two phases coincide).

The expression of the electromagnetic torque of the DFIG depending on flow and stator currents can be written as follows:

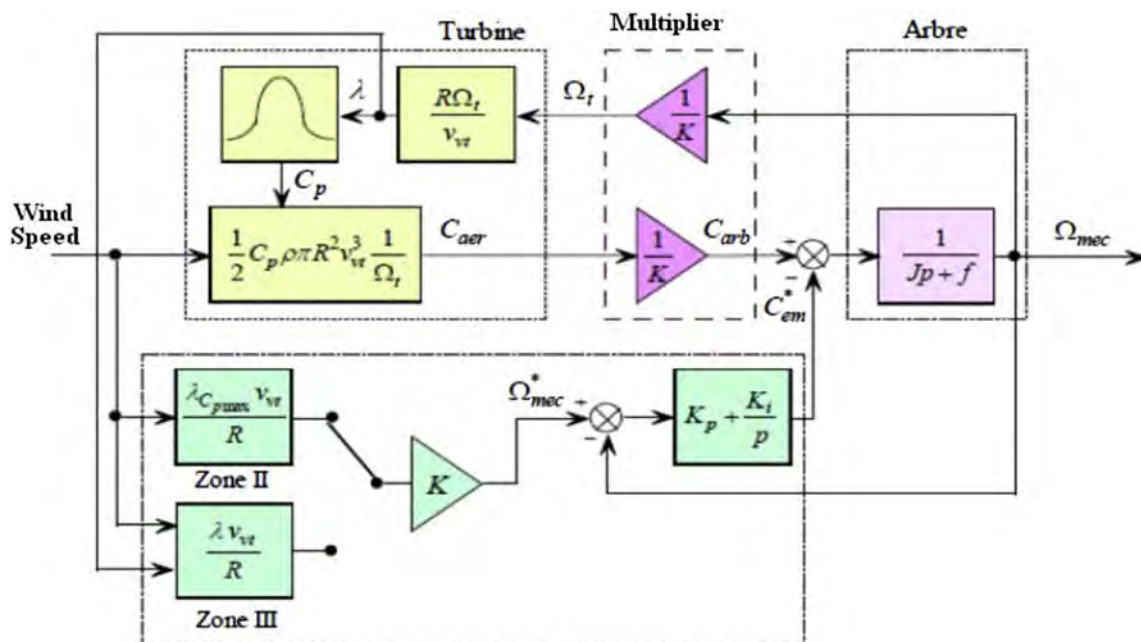


Fig. 5. Block diagram with control of the speed.

$$C_{em} = P(\phi_{ds} \cdot i_{qs} - \phi_{qs} \cdot i_{ds}) \tag{12}$$

With P: number of pole pairs of the DFIG (Fig. 6).

The active and reactive powers stator and rotor of the DFIG are written as follows [10–14]:

$$\begin{cases} P_s = v_{ds} \cdot i_{ds} + v_{qs} \cdot i_{qs} \\ Q_s = v_{qs} \cdot i_{ds} - v_{ds} \cdot i_{qs} \\ P_r = v_{dr} \cdot i_{dr} + v_{qr} \cdot i_{qr} \\ Q_r = v_{qr} \cdot i_{dr} - v_{dr} \cdot i_{qr} \end{cases} \tag{13}$$

5. Backstepping controller applied to DFIG generator

The adaptive Backstepping control approach is a control technique that can effectively linearize a nonlinear system as DFIG in the presence of uncertainties. Unlike other information linearization techniques, adaptive Backstepping has the flexibility to keep useful nonlinearity intact during stabilization. The essence of Backstepping is to stabilize the state of the virtual control. Therefore, it generates a corresponding error variable that can be stabilized by carefully selecting the appropriate control inputs. These inputs can be determined from the analysis of Lyapunov stability.

From (10) it is clear that the dynamic model of the DFIG is highly non-linear due to the coupling between the speed and the electric currents. According to the vector control principle, the direct axis current i_d is always forced to be zero in order to orient all the linkage flux in the d axis and achieve maximum torque per ampere.

$$\begin{aligned} \frac{d\phi_{rd}}{dt} &= V_{rd} + \left(\frac{R_r \cdot M}{\sigma \cdot L_s \cdot L_r}\right) \phi_{sd} - \left(\frac{R_r}{\sigma \cdot L_r}\right) \phi_{rd} + \omega_r \cdot \phi_{rq} \\ \frac{d\phi_{rq}}{dt} &= V_{rq} + \left(\frac{R_r \cdot M}{\sigma \cdot L_s \cdot L_r}\right) \phi_{sq} - \left(\frac{R_r}{\sigma \cdot L_r}\right) \phi_{rq} - \omega_r \cdot \phi_{rd} \\ \frac{d\phi_{sd}}{dt} &= V_{sd} + \left(\frac{R_s \cdot M}{\sigma \cdot L_s \cdot L_r}\right) \phi_{rd} - \left(\frac{R_s}{\sigma \cdot L_s}\right) \phi_{sd} + \omega_s \cdot \phi_{sq} \\ \frac{d\phi_{sq}}{dt} &= V_{sq} + \left(\frac{R_s \cdot M}{\sigma \cdot L_s \cdot L_r}\right) \phi_{rq} - \left(\frac{R_s}{\sigma \cdot L_s}\right) \phi_{sq} - \omega_s \cdot \phi_{sd} \end{aligned} \tag{14}$$

It is obvious that the dynamic model is highly nonlinear due to the coupling between the velocity and magnetic flux. For this the study of stability of the system characterized by:

$[X] = [\phi_{rd} \ \phi_{rq} \ \phi_{sd} \ \phi_{sq} \ \Omega]^T$: is the state vector (the flux and speed are measurable).

$[U] = [V_{rd} \ V_{rq} \ V_{sd} \ V_{sq}]^T$: is the control variable (voltage stator and rotor).

The Lyapunov function is dividing in two steps, one for the control of the speed and the other for the control of the flux.

5.1. Backstepping controller speed

The first step of the Backstepping control is defined Lag error of the state variable by the following calculation:

$$e_\Omega = \Omega_{ref} - \Omega \tag{15}$$

Its derivative gives:

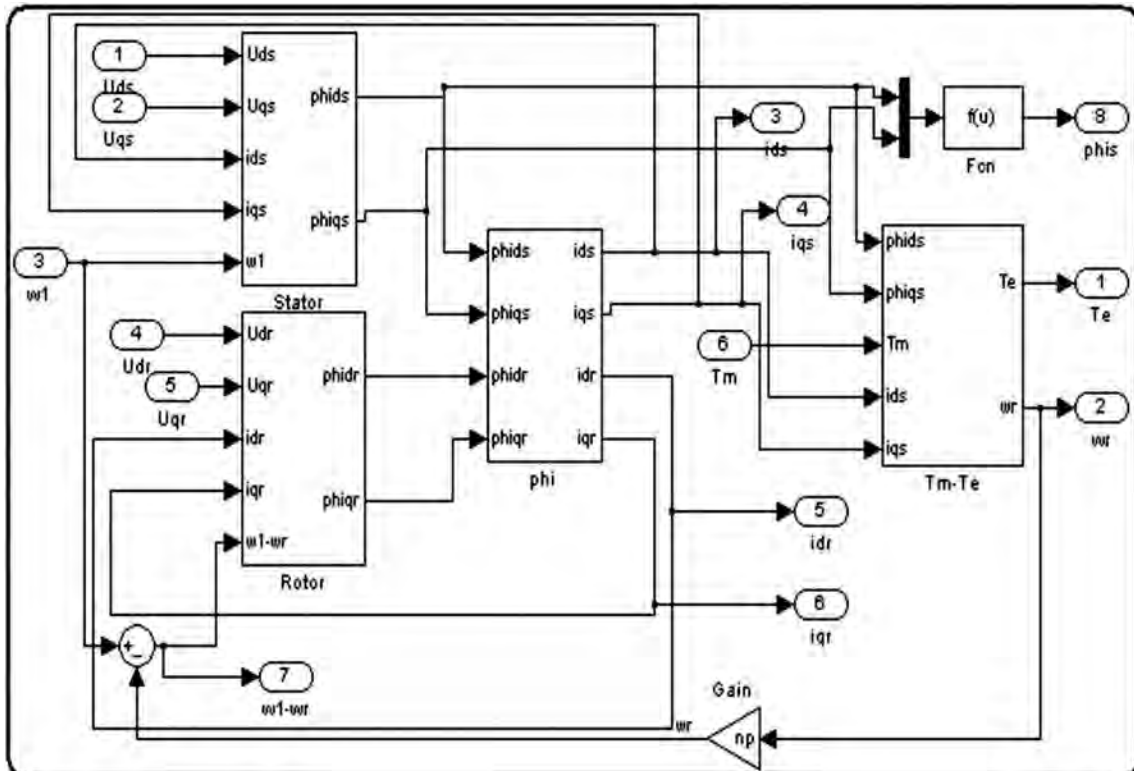


Fig. 6. DFIG Model for wind-turbine.

$$\dot{e}_\Omega = \frac{de_\Omega}{dt} = \dot{\Omega}_{ref} - \dot{\Omega} \quad (16)$$

with:

$$\dot{\Omega} = \left(\frac{P(1-\sigma)}{J \cdot \sigma \cdot M} \right) (\phi_{rd} \cdot \phi_{sq} - \phi_{rq} \cdot \phi_{sd}) - \frac{f}{J} \Omega - \frac{C_r}{J} \quad (17)$$

One finds:

$$\dot{e}_\Omega = \dot{\Omega}_{ref} - \left(\frac{P(1-\sigma)}{J \cdot \sigma \cdot M} \right) (\phi_{rd} \cdot \phi_{sq} - \phi_{rq} \cdot \phi_{sd}) - \frac{f}{J} \Omega - \frac{C_r}{J} \quad (18)$$

With the application the principles of rotor flux orientation:

$$\begin{cases} \phi_{sd} = 0 \\ \phi_{rq} = 0 \end{cases}$$

It results in the following expression:

$$\dot{e}_\Omega = \dot{\Omega}_{ref} - \left(\frac{P(1-\sigma)}{J \cdot \sigma \cdot M} \right) (\phi_{rd} \cdot \phi_{sq}) + \frac{f}{J} \Omega + \frac{C_r}{J} \quad (19)$$

Subsequently we define the Lyapunov function of the form:

$$V_1 = \frac{1}{2} e_\Omega^2 \quad (20)$$

Its derivative gives:

$$\begin{aligned} \dot{V}_1 &= e_\Omega \dot{e}_\Omega \\ \dot{V}_1 &= e_\Omega \left(\dot{\Omega}_{ref} - \left(\frac{P(1-\sigma)}{J \cdot \sigma \cdot M} \right) (\phi_{rd} \cdot \phi_{sq}) + \frac{f}{J} \Omega + \frac{C_r}{J} \right) \end{aligned} \quad (21)$$

Using the Backstepping design method, to ensure the stability of the sub system, for this we need to make equation (19) more negative, we consider the flux ϕ_{rd} , ϕ_{sq} as virtual inputs of our system (12) and define the following equations [9]:

$$\begin{aligned} \dot{V}_2 &= -K_\Omega e_\Omega - K_1 e_1 - K_2 e_2 - K_3 e_3 - K_4 e_4 + e_\Omega \left(K_\Omega e_\Omega - \left(\frac{P(1-\sigma)}{J \cdot \sigma \cdot M} \right) (\phi_r \cdot \phi_s) + \frac{f}{J} \Omega + \frac{C_r}{J} \right) + \\ &e_1 \left(K_1 e_1 + \phi_r - V_{rd} - \left(\frac{R_r \cdot M}{\sigma \cdot L_s \cdot L_r} \right) \phi_{sd} + \left(\frac{R_r}{\sigma \cdot L_r} \right) \phi_{rd} - \omega_r \cdot \phi_{rq} \right) + e_2 \left(K_2 e_2 - V_{rq} - \left(\frac{R_r \cdot M}{\sigma \cdot L_s \cdot L_r} \right) \phi_{sq} + \left(\frac{R_r}{\sigma \cdot L_r} \right) \phi_{rq} + \omega_r \cdot \phi_{rd} \right) \\ &e_3 \left(K_3 e_3 - V_{sd} - \left(\frac{R_s \cdot M}{\sigma \cdot L_s \cdot L_r} \right) \phi_{rd} + \left(\frac{R_s}{\sigma \cdot L_s} \right) \phi_{sd} - \omega_s \cdot \phi_{sq} \right) + e_4 \left(K_4 e_4 + \phi_s - V_{sq} - \left(\frac{R_s \cdot M}{\sigma \cdot L_s \cdot L_r} \right) \phi_{rq} + \left(\frac{R_s}{\sigma \cdot L_s} \right) \phi_{sq} + \omega_s \cdot \phi_{sd} \right) \end{aligned} \quad (28)$$

$$\begin{cases} \phi_{rd_ref} = \phi_r \\ \phi_{sq_ref} = \frac{1}{\left(\frac{P(1-\sigma)}{J \cdot \sigma \cdot M} \right) \cdot \phi_{rd_ref}} \left(K_\Omega e_\Omega + \frac{f}{J} \Omega + \frac{C_r}{J} \right) \end{cases} \quad (22)$$

With K_Ω this is a positive constant.

We substitute equation (20) in the derivative of the Lyapunov function equation V_1 (19) and assuming that Ω_{ref} is constant we have the negativity of the function as:

$$\dot{V}_1 = -K_\Omega e_\Omega^2 \leq 0 \quad (23)$$

Whence the asymptotic stability of the origin of the equation system (12)

5.2. Backstepping controller flux

The objective of the section is the elimination the flux regulators by calculated of the control voltages and for this we define the following errors:

$$\begin{cases} e_1 = \phi_{rd_ref} - \phi_{rd} \\ e_2 = \phi_{rq_ref} - \phi_{rq} \\ e_3 = \phi_{sd_ref} - \phi_{sd} \\ e_4 = \phi_{sq_ref} - \phi_{sq} \end{cases} \quad (24)$$

Its derivative is:

$$\begin{cases} \dot{e}_1 = \dot{\phi}_{rd_ref} - \dot{\phi}_{rd} \\ \dot{e}_2 = \dot{\phi}_{rq_ref} - \dot{\phi}_{rq} \\ \dot{e}_3 = \dot{\phi}_{sd_ref} - \dot{\phi}_{sd} \\ \dot{e}_4 = \dot{\phi}_{sq_ref} - \dot{\phi}_{sq} \end{cases} \quad (25)$$

The results of the derivative of equation (32) are:

$$\begin{cases} \dot{e}_1 = \dot{\phi}_r - V_{rd} - \left(\frac{R_r \cdot M}{\sigma \cdot L_s \cdot L_r} \right) \phi_{sd} + \left(\frac{R_r}{\sigma \cdot L_r} \right) \phi_{rd} - \omega_r \cdot \phi_{rq} \\ \dot{e}_2 = -V_{rq} - \left(\frac{R_r \cdot M}{\sigma \cdot L_s \cdot L_r} \right) \phi_{sq} + \left(\frac{R_r}{\sigma \cdot L_r} \right) \phi_{rq} + \omega_r \cdot \phi_{rd} \\ \dot{e}_3 = -V_{sd} - \left(\frac{R_s \cdot M}{\sigma \cdot L_s \cdot L_r} \right) \phi_{rd} + \left(\frac{R_s}{\sigma \cdot L_s} \right) \phi_{sd} - \omega_s \cdot \phi_{sq} \\ \dot{e}_4 = \dot{\phi}_s - V_{sq} - \left(\frac{R_s \cdot M}{\sigma \cdot L_s \cdot L_r} \right) \phi_{rq} + \left(\frac{R_s}{\sigma \cdot L_s} \right) \phi_{sq} + \omega_s \cdot \phi_{sd} \end{cases} \quad (26)$$

The laws of real machine control are V_{sd} , V_{sq} , V_{rd} and V_{rq} appear in equation (33), then to analyze the stability of this system, we define a new Lyapunov function final V_2 is given by the following form:

$$V_2 = \frac{1}{2} (e_\Omega^2 + e_1^2 + e_2^2 + e_3^2 + e_4^2) \quad (27)$$

The result of the derivative of equation (24) is:

With K_1 , K_2 , K_3 and K_4 are positive constants. Extracted from equation (25) expressions the controls voltages V_{sd} , V_{sq} , V_{rq} and V_{rd} as following:

$$\begin{cases} V_{rd} = \left(K_1 e_1 + \dot{\phi}_r - \left(\frac{R_r \cdot M}{\sigma \cdot L_s \cdot L_r} \right) \phi_{sd} + \left(\frac{R_r}{\sigma \cdot L_r} \right) \phi_{rd} - \omega_r \cdot \phi_{rq} \right) \\ V_{rq} = e_2 \left(K_2 e_2 - \left(\frac{R_r \cdot M}{\sigma \cdot L_s \cdot L_r} \right) \phi_{sq} + \left(\frac{R_r}{\sigma \cdot L_r} \right) \phi_{rq} + \omega_r \cdot \phi_{rd} \right) \\ V_{sd} = e_3 \left(K_3 e_3 - \left(\frac{R_s \cdot M}{\sigma \cdot L_s \cdot L_r} \right) \phi_{rd} + \left(\frac{R_s}{\sigma \cdot L_s} \right) \phi_{sd} - \omega_s \cdot \phi_{sq} \right) \\ V_{sq} = e_4 \left(K_4 e_4 + \dot{\phi}_s - \left(\frac{R_s \cdot M}{\sigma \cdot L_s \cdot L_r} \right) \phi_{rq} + \left(\frac{R_s}{\sigma \cdot L_s} \right) \phi_{sq} + \omega_s \cdot \phi_{sd} \right) \end{cases} \quad (29)$$

This equation (26) implies the negativity of the following Lyapunov function V_2 :

$$V_2 = -K_\Omega e_\Omega - K_1 e_1 - K_2 e_2 - K_3 e_3 - K_4 e_4 \leq 0 \quad (30)$$

5.3. Estimation and observation of parameters DFIG

In the previous equations, the control laws are developed under the assumption that the machine parameters are known and invariants. This assumption is not always true, because, the stator and rotor resistance are varied with temperature, also for the coefficient cyclic inductance of the stator and the rotor. The adaptive Backstepping control takes account of these parametric variations, there are estimated by other parameter same as in equation (17), we do not know the exact value of the load torque \hat{C}_r ; it will be replaced by its estimated \hat{C}_r [15].

$$\hat{\phi}_{rd_ref} = \frac{1}{\left(\frac{P(1-\hat{\sigma})}{J \cdot \hat{\sigma} \cdot M}\right) \cdot \phi_{sd_ref}} \left(K_\Omega e_\Omega + \frac{f}{J} \Omega + \frac{\hat{C}_r}{J} \right) \quad (31)$$

From this relation (31), we deduce the dynamics of the speed error as follows:

$$\dot{e}_\Omega = \left(\frac{P(1-\hat{\sigma})}{J \cdot \hat{\sigma} \cdot M}\right) (\phi_{rd} \cdot \phi_{sq}) + \frac{f}{J} \Omega + \frac{\hat{C}_r}{J} \quad (32)$$

For simplicity the equation (30) we write:

$$\hat{a}_1 = \left(\frac{P(1-\hat{\sigma})}{J \cdot \hat{\sigma} \cdot M}\right)$$

The equation becomes:

$$\dot{e}_\Omega = -\hat{a}_1 (\phi_{rd} \cdot \phi_{sq}) + \frac{f}{J} \Omega + \frac{\hat{C}_r}{J} \quad (33)$$

The new results estimated the parameters of the equation (26) are written:

$$V_2 = \frac{1}{2} \left(e_\Omega^2 + e_1^2 + e_2^2 + e_3^2 + e_4^2 + \frac{\tilde{C}_r^2}{\gamma_1} + \frac{\tilde{a}_1^2}{\gamma_2} + \frac{\tilde{a}_2^2}{\gamma_3} + \frac{\tilde{a}_3^2}{\gamma_4} + \frac{\tilde{a}_4^2}{\gamma_5} \right) \quad (34)$$

The derivative of V_2 is:

$$\dot{V}_2 = \left(e_\Omega \dot{e}_\Omega + e_1 \dot{e}_1 + e_2 \dot{e}_2 + e_3 \dot{e}_3 + e_4 \dot{e}_4 + \frac{\tilde{C}_r \dot{\tilde{C}}_r}{\gamma_1} + \frac{\tilde{a}_1 \dot{\tilde{a}}_1}{\gamma_2} + \frac{\tilde{a}_2 \dot{\tilde{a}}_2}{\gamma_3} + \frac{\tilde{a}_3 \dot{\tilde{a}}_3}{\gamma_4} + \frac{\tilde{a}_4 \dot{\tilde{a}}_4}{\gamma_5} + \frac{\tilde{a}_5 \dot{\tilde{a}}_5}{\gamma_5} \right) \quad (35)$$

Finally, the control laws are now developed as follows:

$$\begin{cases} V_{rd} = (K_1 e_1 + \dot{\phi}_r - \hat{a}_2 \phi_{sd} + \hat{a}_3 \phi_{rd} - \omega_r \cdot \phi_{rq}) \\ V_{rq} = e_2 (K_2 e_2 - \hat{a}_2 \phi_{sq} + \hat{a}_3 \phi_{rq} + \omega_r \cdot \phi_{rd}) \\ V_{sd} = e_3 (K_3 e_3 - \hat{a}_4 \phi_{rd} + \hat{a}_5 \phi_{sd} - \omega_s \cdot \phi_{sq}) \\ V_{sq} = e_4 (K_4 e_4 + \dot{\phi}_s - \hat{a}_4 \phi_{rq} + \hat{a}_5 \phi_{sq} + \omega_s \cdot \phi_{sd}) \end{cases} \quad (36)$$

With this calculation, the expression (36) becomes:

$$V_2 = -K_\Omega e_\Omega - K_1 e_1 - K_2 e_2 - K_3 e_3 - K_4 e_4 \leq 0 \quad (37)$$

So the system is globally asymptotically stable in the presence of parametric uncertainties and variables.

6. FPGA-based implementation of an robust backstepping control system

6.1. Development of the implementation

There are several manufacturers of FPGA components such: Actel, Xilinx and Altera ... etc. These manufacturers use different technologies for the implementation of FPGAs. These technologies are attractive because they provide reconfigurable structure that is the most interesting because they allow great flexibility in design. Nowadays, FPGAs offer the possibility to use dedicated blocks such as RAMs, multipliers wired interfaces PCI and CPU cores. The architecture designing was done using with CAD tools. The description is made graphically or via a hardware description language high level, also called HDL (Hardware Description Language). Is commonly used language VHDL and Verilog. These two languages are standardized and provide the description with different levels, and especially the advantage of being portable and compatible with all FPGA technologies previously introduced [7].

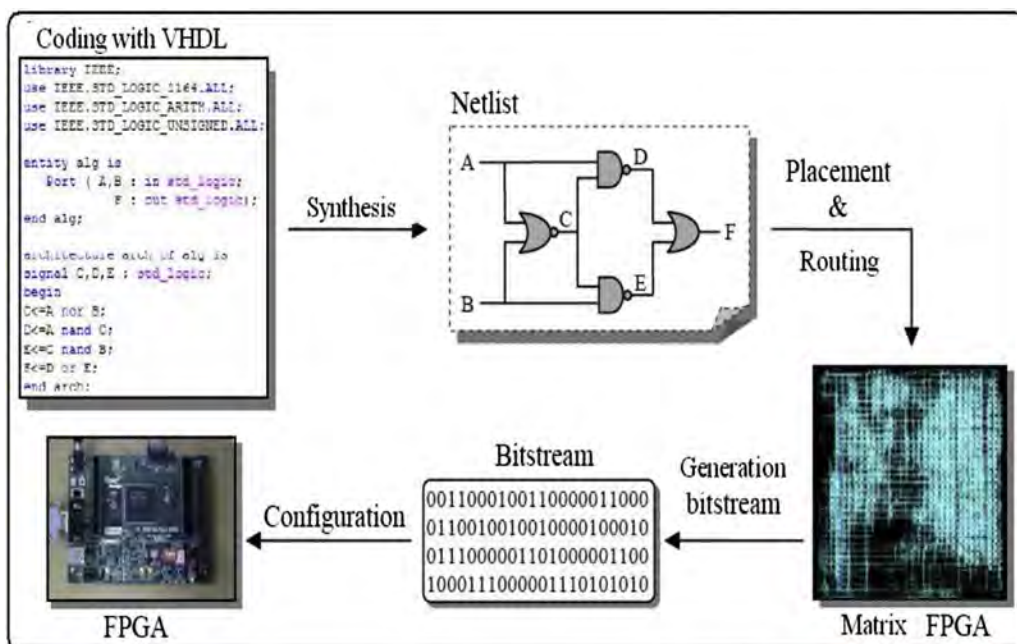


Fig. 7. Programming FPGA devices.

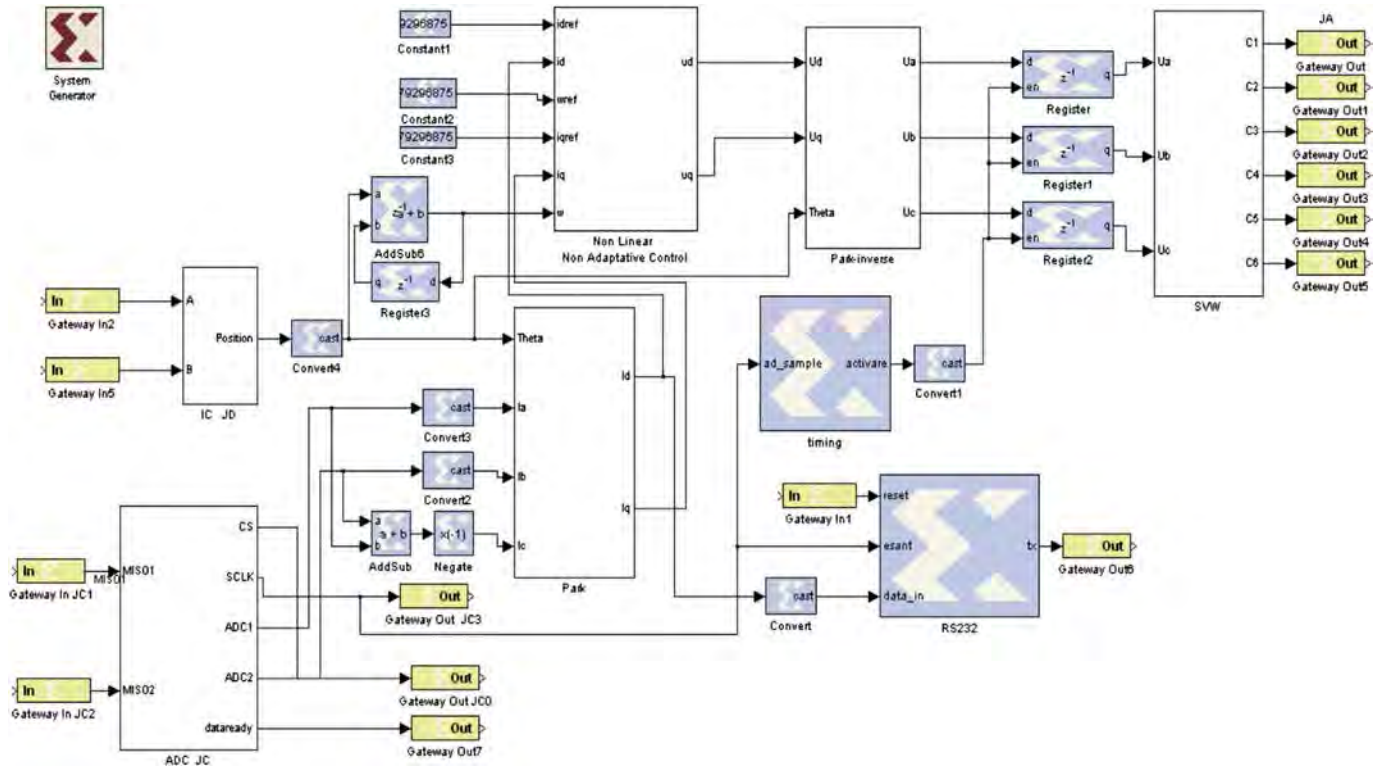


Fig. 8. Functional model for adaptive backstepping controller from SYSTEM GENERATOR.

In this paper an *FPGA XC3S500E* Spartan3E from Xilinx is used. This *FPGA* contains 400,000 logic gates and includes an internal oscillator which issues a 50 MHz frequency clock. The map is composed from a matrix of 5376 slices linked together by programmable connections.

Fig. 7 summarizes the different steps of programming an *FPGA*. The synthesizer generated with *CAD* tools first one Netlist which describes the connectivity of the architecture. Then the placement-routing optimally place components and performs all the routing between different logic. These two steps are used to generate a

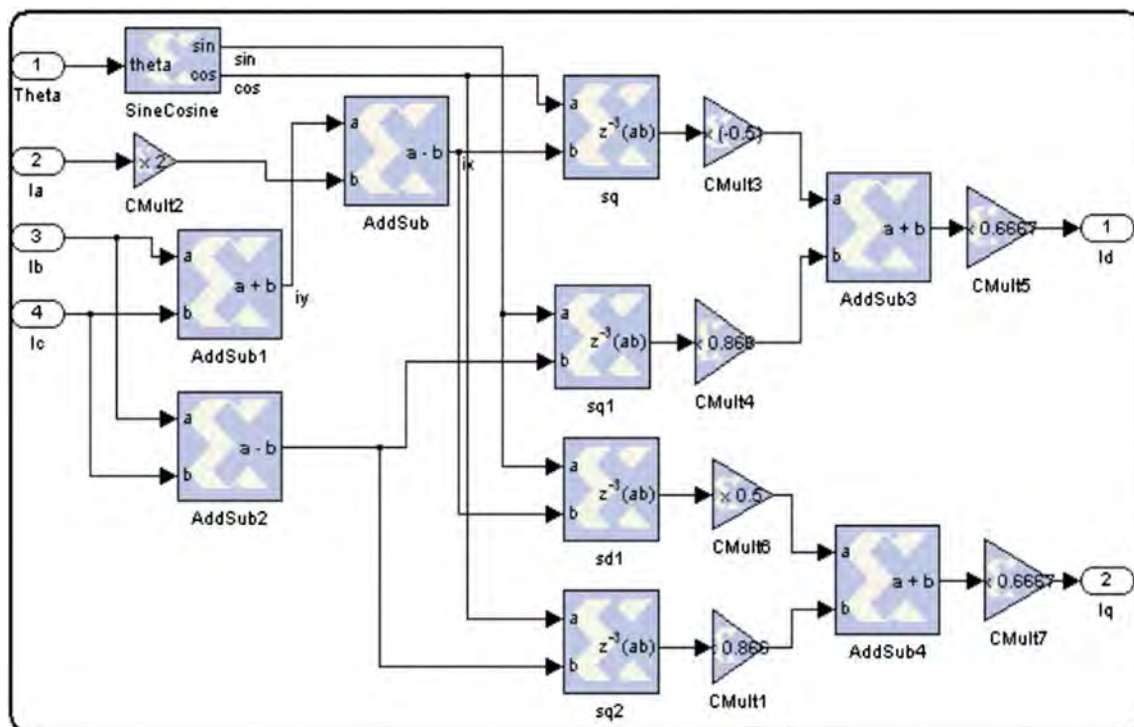


Fig. 9. Park transformation model.

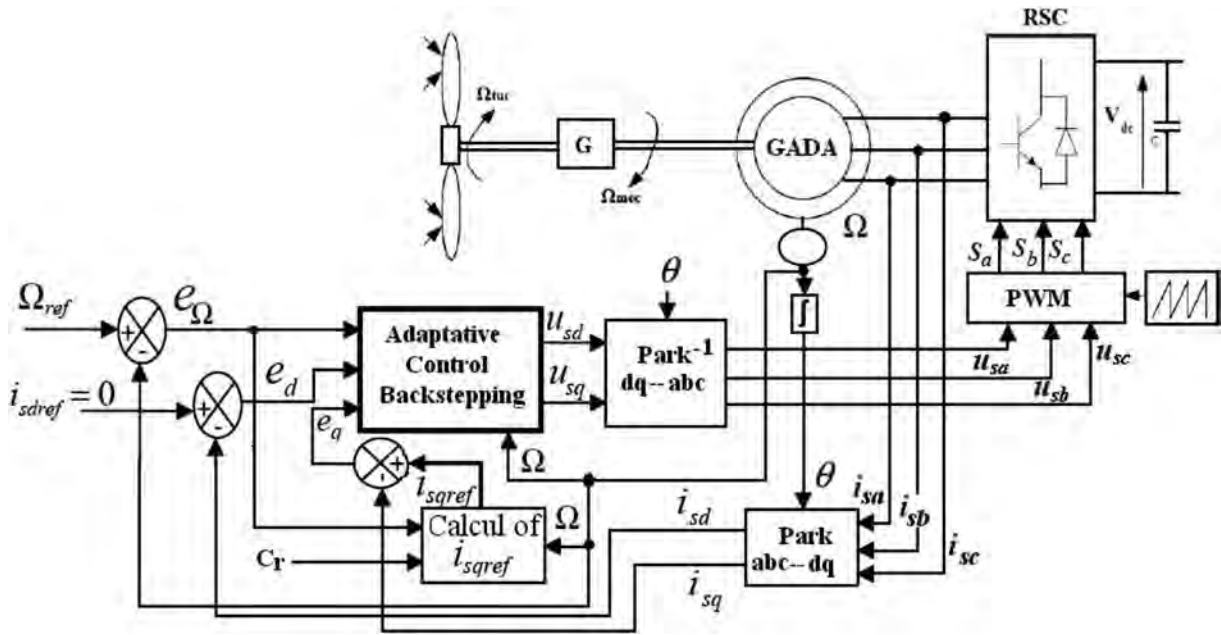


Fig. 10. Simulation scheme of adaptive Backstepping Control applied for DFIG-wind-turbine.

configuration file to be downloaded into the memory of the FPGA. This file is called bitstream. It can be directly loaded into FPGA from a host computer.

In this work an FPGA XC3S500E Spartan3E from Xilinx is used. This FPGA contains 400,000 logic gates and includes an internal oscillator which issues a 50 MHz frequency clock. The map is composed from a matrix of 5376 slices linked together by programmable connections.

6.2. Simulation procedure

The simulation procedure begins by verifying the functionality of the control algorithm by trailing a functional model using Simulink System Generator for Xilinx blocks. For this application, the functional model consists in a Simulink time discretized model of the No adaptive Backstepping algorithm associated with a voltage inverter and DFIG model. Fig. 7 shows

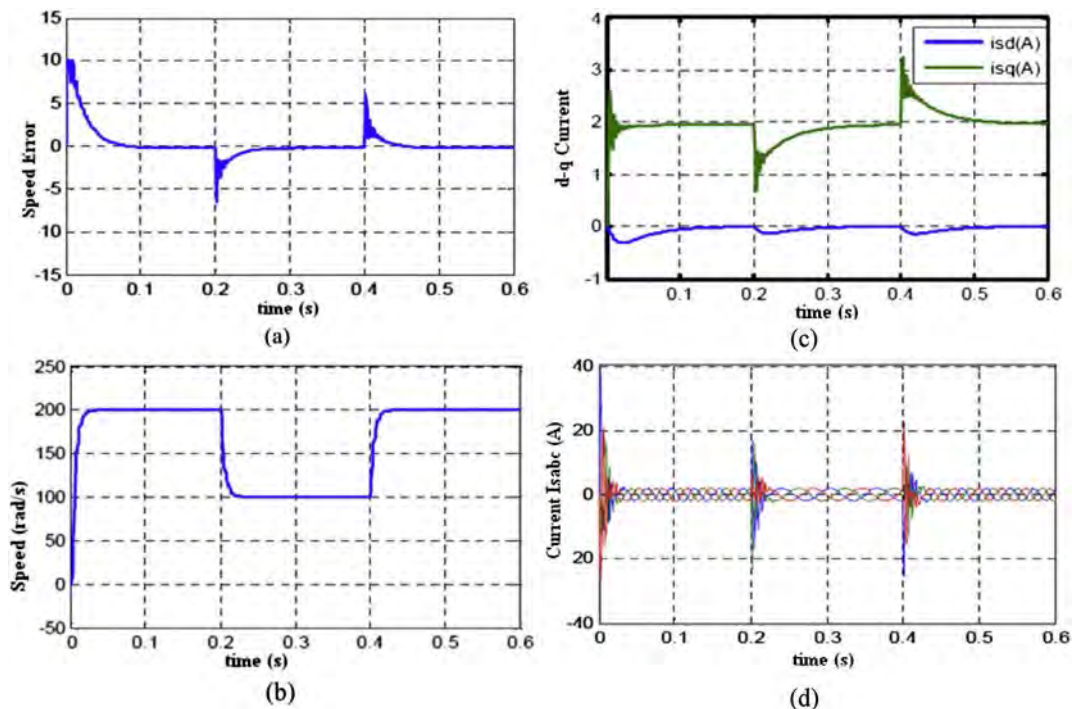


Fig. 11. Test performance of the adaptive controller for trajectory tracking, (a) Speed response trajectory (b) Error Speed response (c) d-q axis current without uncertainties (d) abc axis current.

in detail the programming of the control shown in Fig. 1 in the SYSTEM GENERATOR environment from Xilinx, we will implement it later in the memory of the FPGA for the simulation of DFIG.

The functional model for no adaptative Backstepping Controller from SYSTEM GENERATOR is composed the different blocks:

- The block encoder interface IC allows the adaptation between the FPGA and the acquisition board to iniquity the rotor position of the DFIG,
- The ADC interface allows the connection between the FPGA and the analog-digital converter (ADCS7476MSPS 12-bit A/D) that will be bound by the following two Hall Effect transducers for the acquisition of the stator currents machine,
- The blocks of coordinate's transformation: the transformation of Park Inverse (*abc-to-dq*),
- The blocks of coordinate's transformation: the transformation of Park (*dq-to-abc*),
- The SVW block is the most important, because can provide control pulses to the IGBT voltage inverter in the power section from well-regulated voltages,
- The block for the controller no adaptative Backstepping which is designed to regulate the speed and stator currents of the DFIG,
- Block "Timing" which controls the beginning and the end of each block, which allows the refresh in the voltages reference V_{10} , V_{20} and V_{30} at the beginning of each sampling period,
- The RS232 block allows signal timing and recovery of signals viewed, created by another program on Matlab & Simulink to visualize the desired output signal.

The second step of the simulation is the determination of the suitable sampling period and fixed point format. Fig. 8 gives the specification model of the *abc-to-dq* (park) transformation.

For example, we present the construction of Block Clark's Transformation in the system generator environment from Xilinx, which is characterized by the following system:

$$\begin{bmatrix} V_{sd} \\ V_{sq} \\ V_0 \end{bmatrix} = \sqrt{\frac{2}{3}} \begin{bmatrix} \cos\theta & \cos\left(\theta - \frac{2\pi}{3}\right) & \cos\left(\theta - \frac{4\pi}{3}\right) \\ -\sin\theta & -\sin\left(\theta - \frac{4\pi}{3}\right) & -\sin\left(\theta - \frac{4\pi}{3}\right) \\ \frac{1}{\sqrt{2}} & \frac{1}{\sqrt{2}} & \frac{1}{\sqrt{2}} \end{bmatrix} \begin{bmatrix} V_{sa} \\ V_{sb} \\ V_{qc} \end{bmatrix} \tag{38}$$

The specification model is then used for the definition of the corresponding Data Flow Graph. Fig. 9 shows the DFG corresponding to the Park transformation module.

7. Simulation & results

The overall model of the wind system was simulated in Matlab/Simulink/SimPowerSystems environment. The model includes: wind turbine, Doubly-Fed Asynchronous Generator (DFIG), two power converters that connect the rotor to the grid (GSC and RSC) (Fig. 10).

7.1. DFIG performances

The following results are obtained by choosing the following values:

- ✓ Gains of the control law: $k_\omega = 0.15$, $k_d = 0.01$, $k_q = 0.01$.
- ✓ Adaptation gains: $\gamma_1 = 0.15$, $\gamma_2 = 0.01$, $\gamma_3 = 0.015$.

- Follow of the trajectory (Fig. 11)
- Disturbance rejection (Fig. 12)
- Parametric uncertainties (Figs. 13–15)

7.2. Wind-turbine performances

Using the reduced model, we applied a profile closer to the evolution of the real wind was filtered to suit the slow dynamics of the system studied random wind. The objective is to see the degree of continuing point of maximum power and efficiency of the speed control provided by the backstepping controller.

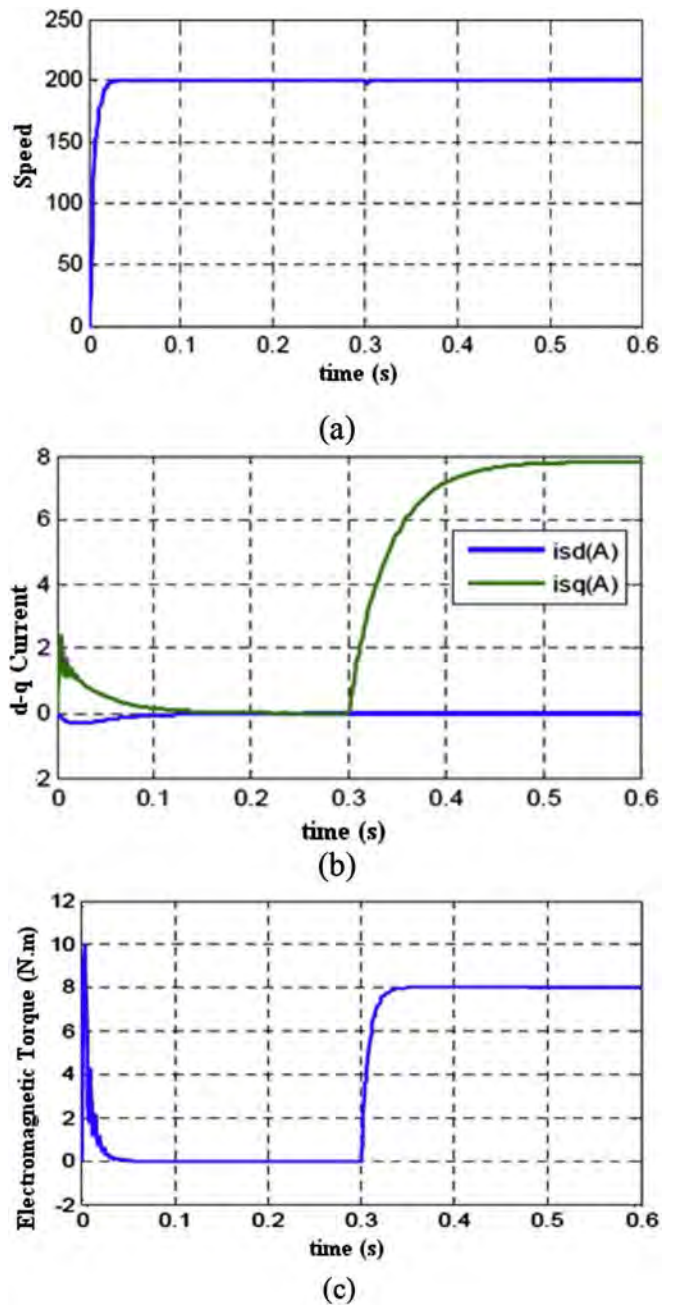


Fig. 12. Test performance of the adaptive controller for rejecting disturbance torque load applied at $t = 0.3$ s. (a)Speed response trajectory (b) d-q axis current without uncertainties (c) Electromagnetic Torque.

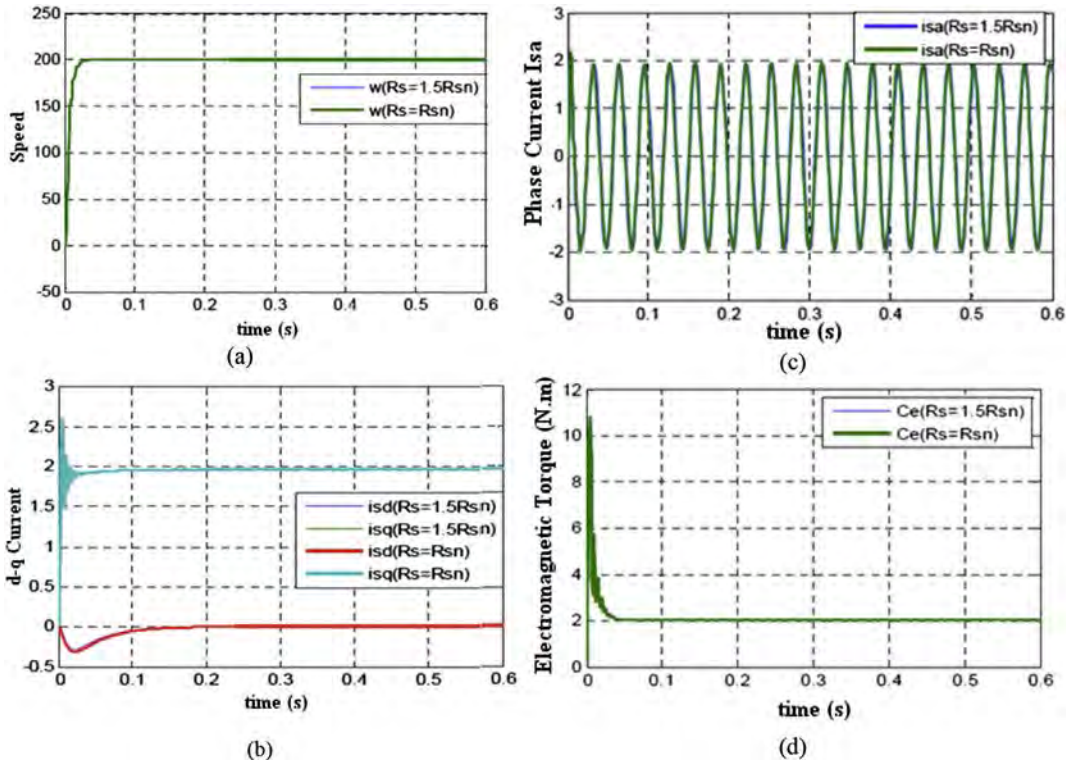


Fig. 13. Test performance of the adaptive controller following a change in R_s . (a) Speed response trajectory (b) d-q axis current without uncertainties (c) Electromagnetic Torque (d) current i_{sa} .

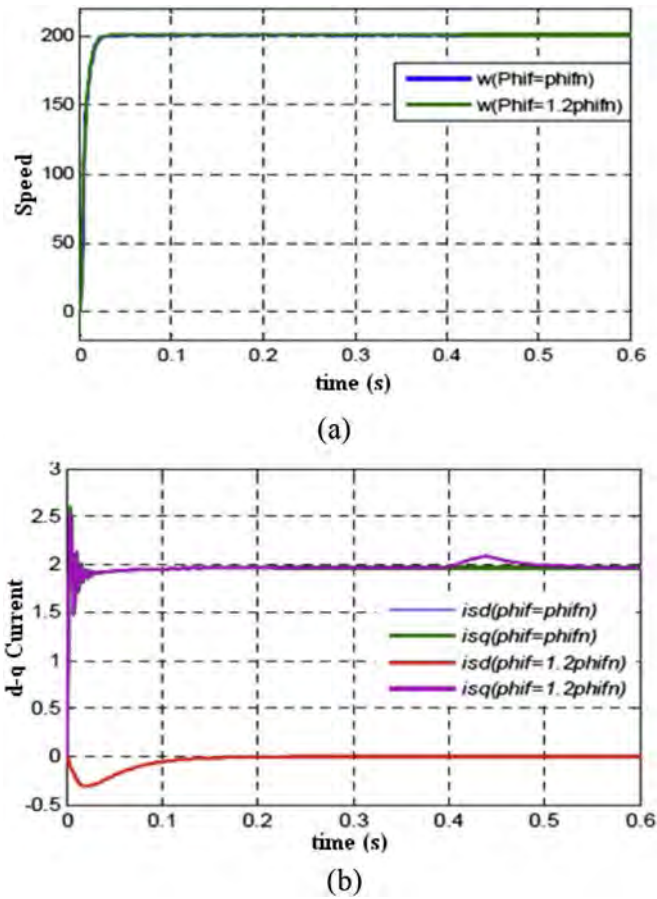


Fig. 14. Test performance of the adaptive controller following a change in ϕ_f . (a) Speed response trajectory (b) d-q axis current without uncertainties.

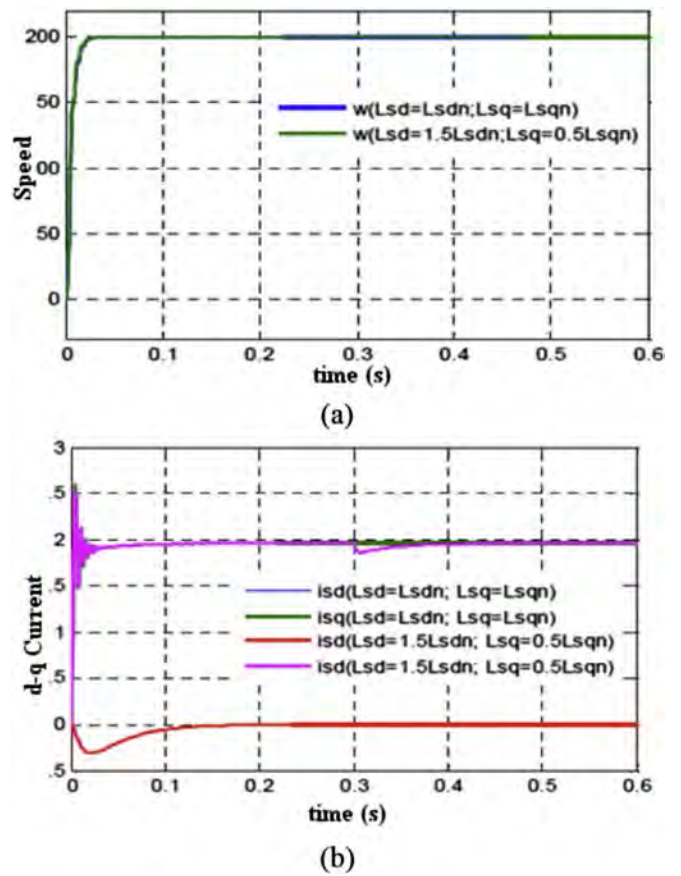


Fig. 15. Test performance of the adaptive controller following a change in L_{sd} and L_{sq} . (a) Speed response trajectory (b) d-q axis current without uncertainties.

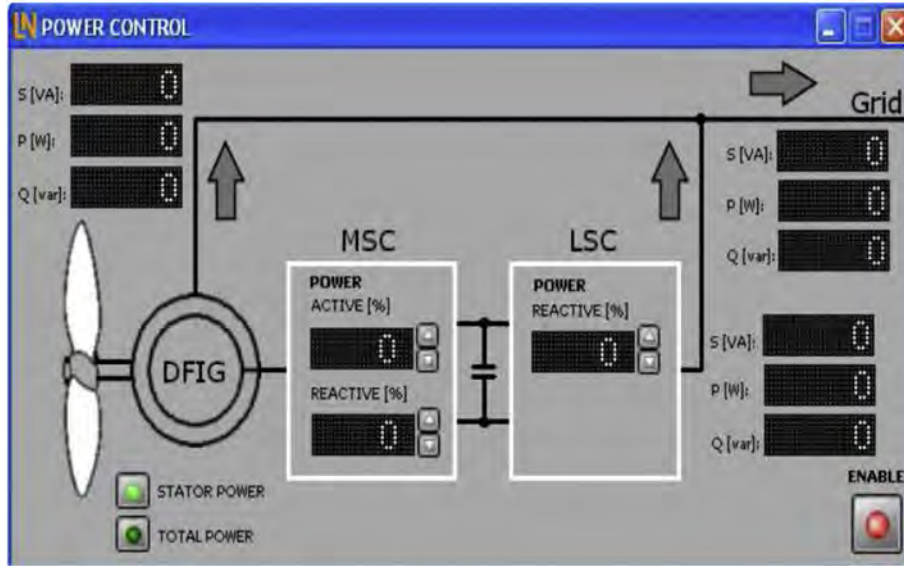


Fig. 16. DFIG-Generator with wind turbine interface.

The following graph shows the function of a wind turbine with asynchronous generator dual power scheme (Fig. 16) (Figs. 17 and 18).

Fig. 19 shows the wind profile filtered and applied to the system in this case.

Fig. 20 shows the results obtained for this application, where the following observations can be distinguished:

- > The specific speed λ and the power coefficient C_p does not change a lot of values, they are almost equal to their optimal values references 9 and 0.4999 successively;
- > The wind power captured follows its optimal reference and has the same shape as the wind profile applied, this rate is also consistent with the wind torque side of the MADA;
- > The speed of the DFIG is the image of wind causing the wind, it properly follows its reference;
- > The shapes of the electromagnetic torque of the DFIG and its reference, are virtually identical, but different from the shape of

the profile of the wind speed due to the dynamic torque due to inertia;

- > The phase shift between the voltage 180° and the stator current phase reflects a production of active power only to the stator as illustrated in figure powers;
- > The shape of the components of the stator flux orientation shows a good flow to ensure vector control well decoupled from the DFIG.

8. Comparison and discussion

In this section, analysis and interpretation of the results obtained from the validation of our order for wind turbine systems is presented, and a comparison with a work of literature that is based on a different type of control systems for wind [16].

The use of the generator DFIG for the production of electrical energy from a wind system has large advantages in terms of production and control. it produces more energy from the stator and

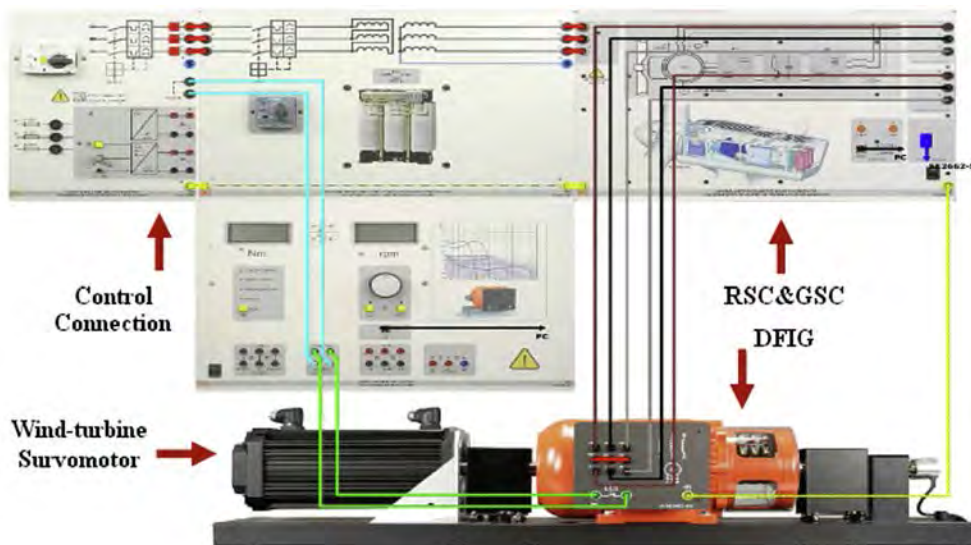


Fig. 17. Benchmark of wind turbine system.

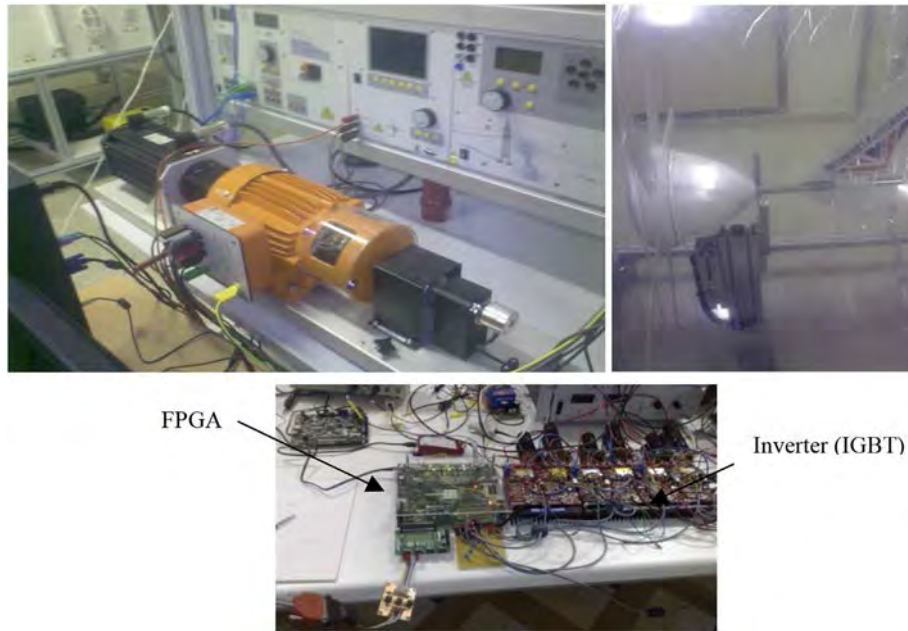


Fig. 18. Experimental benchmark of wind turbine system.

rotor, it also has a big advantage on the robustness and reliability of the system saw the disturbance and the control will be done with a wide feasibility compared with other machine (IM, PMSG).

The paper [16] present a linear control which is based on the sliding mode technique, this is a powerful approach to the control of electric machines especially for the permanent magnet synchronous machine.

This control technique is a major inconvenient, generator modeling is done just in the linear mode, which has no reality, and the results obtained are far from reality.

However, our contribution is based on the application of Backstepping control to improve the performance of wind power system based on DFIG generator. This control strategy is based on the Lyapunov technique that is highly non linear and makes the system non-linear fashion, without forgetting that processed the command with a variance of the parameters of the machine.

The Backstepping adaptive control has the following advantages:

- Ensures asymptotic stability and speed control and direct current;
- Fixed speed error vector;

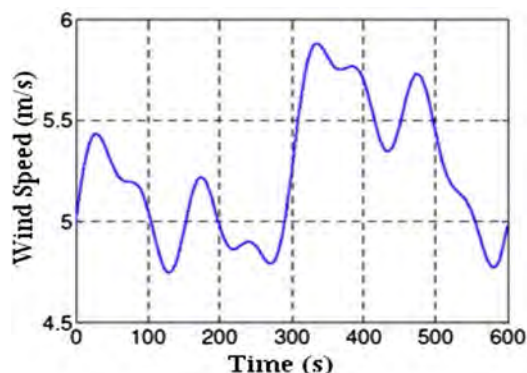


Fig. 19. Profile applied to random wind Wind-turbine.

- Very good dynamics during transient;
- The switching frequency is limited to half the sampling frequency;
- The parameters of the control algorithm are independent of machine parameters of the sampling period used;

The Backstepping adaptive control has the following inconvenient:

- The general structure of the control algorithm is complex to implement;
- Dynamic transient is slower;

The wind speed profile used in this work is purely instantaneous, but with average speed for the use of a small wind turbine in our laboratory (200 kW). But the model used is valid for all types of wind turbines.

Fig. 20 shows the different performance of the wind system, which show the robustness and followed the given path, specific speed and power coefficient proportionally vary with wind speed which shows the reliability of the system.

The speed of rotation of the machine and the turbine are of less oscillations and greater reliability relative to the input speed.

The active and reactive power is dedicated power, and we note that almost null reactive power, which makes the system more robust.

The voltage and current at the output of the wind system are purely sinusoidal with a constant frequency and present no problems when connecting to the grid.

In Ref. [16] paper, the performances of the systems (turbine speed and power) are not consistent and do not follow the wind speed reference.

Figs. 7 and 8 present a lot of oscillations in the speed curve, implying less robust.

Our approach is a further contribution to the application of nonlinear controls on wind systems based on DFIG generator.

The results obtained show the reliability and robustness of the proposed control and provides better control for injecting power into the grid.

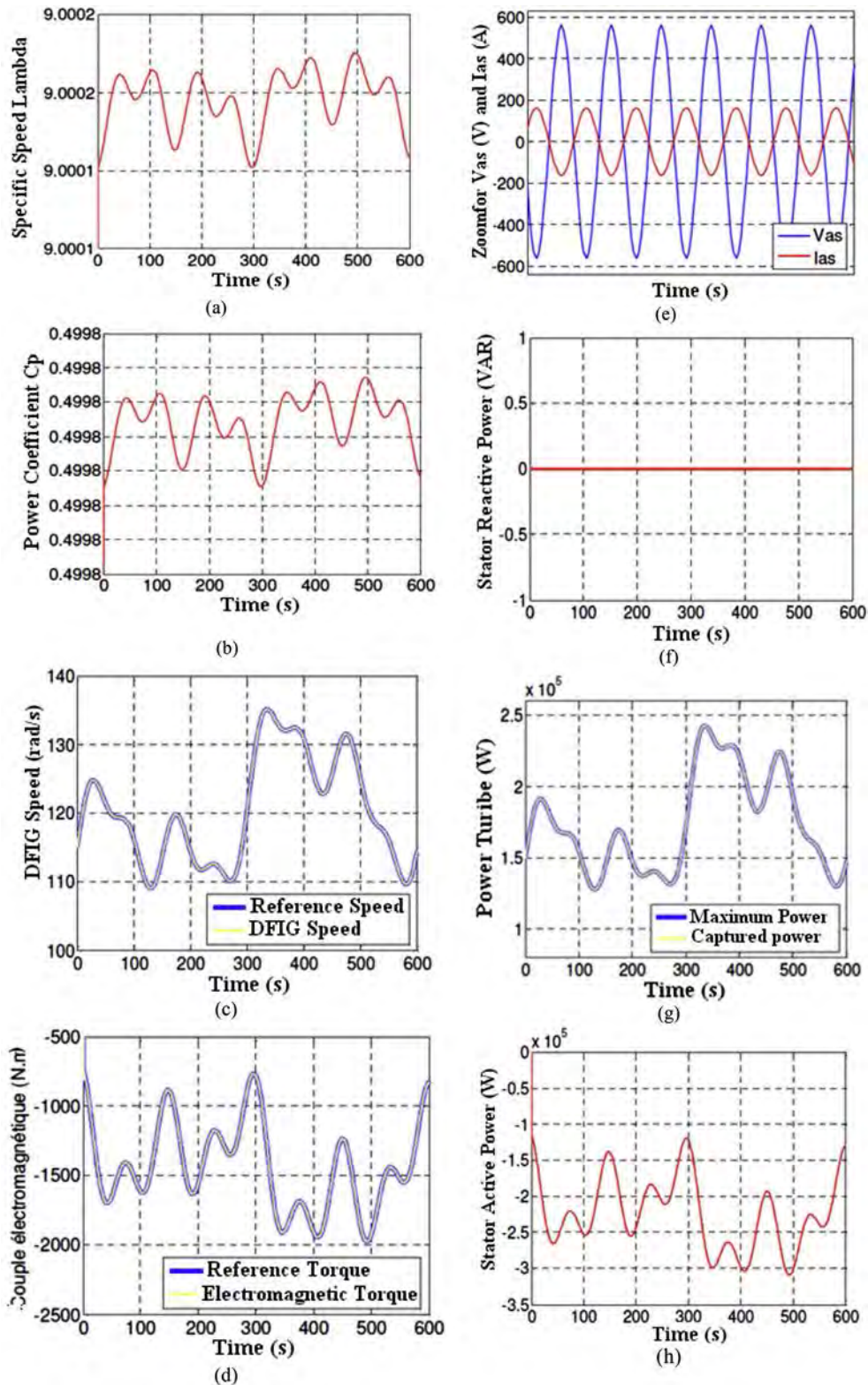


Fig. 20. The Simulation results of the asynchronous wind generator dual power and stator flux oriented, with a Backstepping controller (Case scale model of the DFIG and profile of random wind).

9. Conclusion

This work has been devoted to modeling, simulation and analysis of a wind turbine operating at variable speed. A stable

operation of the wind energy system is obtained with the application of nonlinear Backstepping Adaptive control. The overall operation of the wind turbine and its control system were illustrated by responses to transient and permanent control systems.

Generator supplied power to the network with an active power whatever the mode of operation. The wind generator has been tested and modeled with a variable speed operation for a power of 200 kW. Simulation results show that the proposed wind system and is feasible and has many advantages.

References

- [1] Ackermann T, Soder L. An overview of wind energy-status 2002. *Renew Sustain Energy Rev* 2002;6(1–2):67–127.
- [2] Burton T, Sharpe D, Jenkins N, Bossanyi E. *Wind energy handbook*. John Wiley&Sons, Ltd; 2001.
- [3] Kling WL, Sootweg JG. Wind turbines as power plants. In: *Proceeding of the IEEE/Cigre workshop on wind power and the impacts on power systems*; 17–18 June 2002 [Oslo, Norway].
- [4] Seyoum D, Grantham C. Terminal voltage control of a wind turbine driven isolated induction generator using stator oriented field control. *IEEE Trans Ind Appl* September 2003:846–52.
- [5] Davigny A. *Participation aux services système de fermes éoliennes à vitesse variable intégrant un stockage inertiel d'énergie* [Thèse de Doctorat]. France: USTL Lille; 2007.
- [6] Ghedamsi K. *Contribution à la modélisation et la commande d'un convertisseur direct de fréquence. Application à la conduite de la machine asynchrone* [Thèse de Doctorat]. Algérie: ENP Alger; 2008.
- [7] Bossoufi B, Karim M, Ionita S, Lagrioui A. Nonlinear non adaptive backstepping with sliding-mode torque control approach for PMSM motor. *J J Electr Syst JES* June 2012;8(2):236–48.
- [8] Yu X, Strunz K. Combined long-term and short term access storage for sustainable energy system 2004. *IEEE power engineering society general meeting*, vol. 2; 10 June 2004. p. 1946–51.
- [9] Ben Elghali SE. *Modélisation et Commande d'une hydrolienne Equipée d'une génératrice asynchrone double alimentation*. JGGE'08. 16–17 Décembre 2008 [Lyon (France),S].
- [10] Aïmani E. *Modélisation de différentes technologies d'éoliennes intégrées dans un réseau de moyenne tension* [Thèse de Doctorat]. France: École Centrale de Lille; 2004.
- [11] Yao X, Yi C, Ying D, Guo J, Yang L. The grid-side PWM converter of the wind power generation system based on fuzzy sliding mode control. In: *Advanced intelligent mechatronics, IEEE; 2008* [Xian (Chine)].
- [12] Bossoufi B, Karim M, Ionita S, Lagrioui A. DTC control based artificial neural network for high performance PMSM drive. *J Theor Appl Inform Technol JATIT* 30th November 2011;33(2):165–76.
- [13] Bossoufi B, Karim M, Ionita S, Lagrioui A. Indirect sliding mode control of a permanent magnet synchronous machine: FPGA-based implementation with Matlab & Simulink simulation. *J Theor Appl Inform Technol JATIT* 15th July 2011;29(1):32–42.
- [14] Boyette A. *Contrôle-commande d'un générateur asynchrone à double alimentation avec système de stockage pour la production éolienne* [Thèse de Doctorat]. 2006. Nancy (France).
- [15] Bossoufi B, Karim M, Ionita S, Lagrioui A. Low-speed sensorless control of PMSM motor drive using a nonlinear approach backstepping control: FPGA-based implementation. *J Theor Appl Inform Technol JATIT* 29th February 2012;36(1):154–66.
- [16] Bekakra Y, Ben Attous D. Sliding mode controls of active and reactive power of a DFIG with MPPT for variable speed wind energy conversion. *Aust J Basic Appl Sci* 2011;5(12):2274–86.